Title	Enhanced dark hydrogen fermentation of Enterobacter aerogenes/HoxEFUYH with carbon cloth
Authors	Cheng, Jun;Li, Hui;Zhang, Jiabei;Ding, Lingkan;Ye, Qing;Lin, Richen
Publication date	2019-01-04
Original Citation	Cheng, J., Li, H., Zhang, J., Ding, L., Ye, Q. and Lin, R. (2019) 'Enhanced dark hydrogen fermentation of Enterobacter aerogenes/HoxEFUYH with carbon cloth', International Journal of Hydrogen Energy, In Press, doi: 10.1016/j.ijhydene.2018.12.080
Type of publication	Article (peer-reviewed)
Link to publisher's version	http://www.sciencedirect.com/science/article/pii/S0360319918340448 - 10.1016/j.ijhydene.2018.12.080
Rights	© 2018 Hydrogen Energy Publications LLC. Published by Elsevier Ltd. All rights reserved. This manuscript version is made available under the CC-BY-NC-ND 4.0 license - http://creativecommons.org/licenses/by-nc-nd/4.0/
Download date	2025-03-18 00:30:48
Item downloaded from	https://hdl.handle.net/10468/7317

Enhanced dark hydrogen fermentation of *Enterobacter aerogenes*/HoxEFUYH with carbon cloth

Jun Cheng [a*], Hui Li [a], Jiabei Zhang [a], Lingkan Ding [a], Qing Ye [a], Richen Lin [b, c]

[a] State Key Laboratory of Clean Energy Utilization, Zhejiang University, Hangzhou 310027, China

[b] MaREI Centre, Environmental Research Institute, University College Cork, Cork, Ireland

[c] School of Engineering, University College Cork, Cork, Ireland

E-mail address:

Prof. Dr. Jun Cheng: juncheng@zju.edu.cn

Hui Li: 11627006@zju.edu.cn

Jiabei Zhang: zhangjiabei@zju.edu.cn

Lingkan Ding: dlkschumi@126.com

Qing Ye: yeqing54321@zju.edu.cn

Dr. Richen Lin: richen.lin@ucc.ie

[*] Corresponding author：Prof. Dr. Jun Cheng, State Key Laboratory of Clean Energy Utilization, Zhejiang University, Hangzhou 310027, China. Tel.: +86 571 87952889; fax: +86 571 87951616. E-mail: juncheng@zju.edu.cn

Abstract

Long-range extracellular electron transfer through microbial nanowires is critical for efficient bacterial behaviors. The application of carbon cloth on the dark hydrogen fermentation using transgenic *Enterobacter aerogenes* (*E. aerogenes*/*HoxEFUYH*) was first proposed to enhance hydrogen production from glucose. Scanning electron microscopy images showed that the microbial nanowires between *E. aerogenes*/*HoxEFUYH* cells almost vanished due to the presence of carbon cloth. Approximately 59.1% of microorganisms concentrated in biofilms on the surface of carbon cloth, which probably promoted the intercellular electron transfer. The results from Fourier transform infrared spectra and Excitation Emission Matrix spectra indicated that carbon cloth biofilms primarily included polysaccharide and protein. Moreover, the fluorophore of biofilms (88.1%) was much higher than that of supernatant (11.9%). The analysis of soluble metabolic degradation byproducts revealed that carbon cloth selectively enhanced the acetate pathway ($C_6H_{12}O_6+2H_2O\rightarrow 2CH_3COOH+2CO_2+4H_2$), but weakened the ethanol pathway ($C_6H_{12}O_6\rightarrow 2C_2H_5OH+2CO_2$). With 1.0 g/L carbon cloth, the hydrogen yield increased by 26.6% to 242 mL/g, and the corresponding peak hydrogen production rate increased by 60.3%.

Keywords: Electro-conductive carbon cloth; Transgenic *Enterobacter aerogenes*; Hydrogen fermentation

1. Introduction

Alternative renewable energy has become increasingly important because of the rapid depletion of non-renewable fossil fuels (e.g., coal, petroleum and natural gas) [1]. Hydrogen is a clean carbon-free fuel that plays an important role in reducing greenhouse gas emissions [2]. Currently hydrogen is mainly produced from fossil fuels and water electrolysis [3], which are usually unsustainable, consuming energy and emitting greenhouse gas [4]. Biohydrogen production by dark fermentation offers the advantages of energy-saving, low operating costs, and favorable carbon balances [3, 5]. Facultative anaerobes, such as *Enterobacter*, and strict anaerobes, such as *Clostridium*, are efficient hydrogen producers among a large number of hydrogen-producing microorganisms. *Enterobacter aerogenes* (*E. aerogenes*) shows promising use for dark fermentation due to its high growth and hydrogen production rates [6]. Hydrogen is produced by *E. aerogenes* through the following two pathways [7]: formate decomposition pathway, which evolves hydrogen through formate hydrogenlyase from the formate produced by glycolysis; and nicotinamide adenine dinucleotide (NADH) pathway, which produces hydrogen by hydrogenase through the re-oxidation of NADH produced via glycolysis. Hydrogen production from *E. aerogenes* can be regulated by adding external NADH and NAD^+ [8]. Hydrogenase activity can be enhanced via genetic methods to improve hydrogen production. The hydrogenase genes (*hoxEFUYH*) of *Cyanobacteria Synechocystis* sp. PCC 6803 have been successfully amplified and heterologously expressed in *E. aerogenes*

ATCC13408 to improve hydrogen production [9].

Methods focusing on parameter optimization (e.g., pH, temperature and substrate concentration) and metabolic bioengineering have been extensively investigated to improve the hydrogen yield and production rate of *Enterobacter* strains [6, 10]. However, the hydrogen yield of *E. aerogenes* remains markedly lower than the theoretical hydrogen yield of 4 mol/mol glucose. Various electro-conductive and carbon-based materials, such as metal nanoparticles (NPs) [11-15], biochar [16], and granular activated carbon (GAC) [17], have been recently used to enhance fermentative hydrogen production. Nasy et al. investigated the effect of maghemite on biohydrogen production via dark-photo fermentation and claimed that hydrogen production could be remarkably enhanced with the addition of maghemite NPs by promoting the bioactivity of hydrogen-producing microbes [11]. Gadhe et al. used hematite and nickel oxide NPs to enhance the activity of ferredoxin oxidoreductase, ferredoxin, and hydrogenase by accelerating electron transfer owing to the large specific surface area and quantum size effects of NPs, which in turn stimulated hydrogen production [12]. Beckers et al. studied the improving effects of conductive metal (Pd, Ag, and Cu) and metal oxide (Fe_xO_y) on hydrogen fermentation using *Clostridium butyricum*; these effects are mainly attributed to the enhanced activity of hydrogenase and electron transfer rate to protons to generate molecular hydrogen [13]. Other conductive metal NPs, such as iron, nickel [14] and gold NPs [15], also can enhance fermentative hydrogen production from carbohydrate. Zhang et al. reported

that adding appropriate concentrations of biochar could improve fermentative hydrogen production from glucose by promoting the growth of hydrogen-producing bacteria acting as carriers [16]. Granular activated carbon (GAC) can enhance hydrogen fermentation by facilitating the formation of biofilm and efficient colonization of microbes due to its large surface area [17] . Elreedy et al. noted that biohydrogen production from industrial wastewater could be significantly promoted by nickel-graphene nanocomposite because nickel NPs can provide metal nutrients for the synthesis of [Ni-Fe] hydrogenase, whereas graphene substrate can enhance the efficiency of electron transfer involved in hydrogen production [18]. However, the scalable industrial production, cost, and quality are the most challenging obstacles for the successful applications of these additives (such as metal NPs and graphene) in hydrogen fermentation.

Carbon cloth is an electro-conductive material made of thousands of single carbon fibers (diameter c. 6–10 μm) and has high chemical stability, electrical conductivity, large surface area, and low production cost [19]. The large surface area of carbon cloth facilitates the attachment and immobilization of microorganisms because the carbon particles (diameter c. 1–2 mm) are larger than bacterial cells, thereby offering sufficient attachment surfaces to the cells [20]. Similar to biochar [16], carbon cloth could be favorable to enhance the attachment and growth of hydrogen-producing microbes, thus serving as support carriers to improve biohydrogen production. As an electro-conductive material, carbon cloth can facilitate

the potential electron communication between bacterial cells to reduce protons to molecular hydrogen. However, its application in promoting hydrogen production is poorly studied.

To date, the effective use of conductive carbon cloth on hydrogen production of genetically modified *E. aerogenes* has not been reported yet. The microcosmic characters of biofilms on carbon cloth have not been revealed. In this study, carbon cloth was added to improve fermentative hydrogen production. The innovation and objectives of this study are as follows: (1) compare hydrogen yield and production rate with different additions of electro-conductive carbon cloth and non-conductive cotton cloth in anaerobic digestion of glucose; and (2) analyze the compositions and functional groups of the soluble microbial products (SMPs, mainly contain organic macromolecules that are produced by microorganisms) in carbon cloth biofilm and supernatant.

2. Methods

2.1. Microorganisms, plasmids, and medium

E. aerogenes ATCC13408 was purchased from China General Microbiological Culture Collection Centre. The coding region of the hoxEFUYH genes were amplified from the genome of Synechocystis sp. PCC 6803 with forward (hoxEFUYH-F50-CCCGGGATGACCGTTGCCACCGAT-30) and reverse (hoxEFUYH-R 50-CTCGAGCCATTGACATTGAGTTCTCC-30) primers. The

genetic modification method used was from a previous study [21], and the genetically modified *E. aerogenes* was named *E. aerogenes*/HoxEFUYH. The bacteria were cultivated in Luria Bertani (LB) culture medium which contained 5 g/L yeast extract, 10 g/L peptone, and 10 g/L NaCl. Solid LB medium also contained 20 g/L agar.

2.2. Preparation of carbon cloth and cotton cloth

Carbon cloth (Henghui Woven Carbon Fiber Co., China) was used as conductive material. The electrical resistivity and surface area of carbon cloth are 0.0016 Ω·cm and 8.4 m^2/g, respectively. During carbon cloth manufacturing, the surfaces of carbon fiber are probably polluted by various organics, such as oils, alkaloid, and synthetic resin [22]. Formic acid pretreatment was adopted to rinse the pollutants on the surface of carbon cloth [19]. This process eliminated the nitrogen functional groups such as pyrrole nitrogen and pyridine nitrogen, which hindered the electron transfer between microorganisms and carbon cloth [23]. The raw cloth was cleaned with distilled water, dried, and cut into circles of 2 cm in diameter. For formic acid modification, the raw cloth was soaked in 5 mL of formic acid solution (mass fraction of 44%) for 12 h. The cloth was then rinsed five times with distilled water and dried at 100 °C for 4 h in an air atmosphere prior to subsequent experiments. The dried carbon cloth was autoclaved at 121 ℃ for 15 min. For the control, non-electrical conductive cotton cloth, with surface area and size equivalent to those of carbon cloth, was pretreated similarly before being applied to reactors. The carbon cloth and cotton cloth were subsequently added into the medium that contained *E. aerogenes/HoxEFUYH* under

anaerobic condition.

2.3. Analysis methods

2.3.1. Scanning electron microscopy (SEM) analysis

Electron micrographs of the carbon cloth were obtained under a field emission SEM (Hitachi S3700, Japan) to visualize cell attachment to the carbon cloth. Microorganisms with and without carbon cloth were observed separately. The digital electron micrographs were captured with an accelerating voltage of 15 kV.

2.3.2. Bicinchoninic acid method (BCA) analysis

In brief, 1 mL of the culture medium was removed at 1 h and 96 h of fermentation to quantify the protein content in the supernatant. The entire cloth was separated from the liquid using tweezers to quantify the protein content in carbon cloth and cotton cloth biofilms. Cell protein was extracted from the cloth by soaking it in 1 mL of 0.2 N NaOH at 4 °C for 1 h and shaking every 10 s for 15 min. Afterward, 1 mL of deionized water was added to rinse the cloth, which was then removed. The remaining liquid was frozen at −20 °C for 2 h and then placed in an electric-heated thermostatic water bath at 90 °C for 10 min. The above procedure was repeated thrice. The concentration of extracted protein was quantified using bicinchoninic acid method with bovine serum albumin as the protein standard [24].

2.3.3. Extraction and characterization of soluble microbial products

Soluble microbial products (SMPs) mainly include proteins and polysaccharides. The SMPs in carbon cloth biofilms were extracted. Carbon cloth was removed from *E. aerogenes/HoxEFUYH* on the last day of fermentation. The biological membrane was

scraped off the surface and placed in a centrifuge tube. The carbon cloth was then washed with deionized water to rinse the attached SMPs. The centrifuge tube remained vibrating on a vortex generator for 10 min to crush the biofilm and completely dissolve the SMPs. The mixture was then centrifuged at 7500 rpm for 10 min. The SMPs in supernatant were obtained using an acetate fiber microfiltration membrane (0.45 μm).

A Fourier transform infrared spectra (FTIR, Nicolet 5700, USA) was used to observe the difference in the chemical composition and functional groups between the SMPs in carbon cloth biofilms and in supernatant. The SMPs were supplemented with acetone and placed in the refrigerator at 4 °C for 24 h. The sediments were separated and then vacuum dried at 60 °C for 12 h to obtain the dried SMP samples, which were pulverized and then prepared using the potassium bromide (KBr) pellet method. Infrared spectra were measured using a FTIR at room temperature. Each spectrum was obtained from 400 cm^{-1} to 4,000 cm^{-1} [25].

The compositions of the SMP solution were characterized by fluorescence excitation emission matrix spectra (EEM) using a Cary Eclipse fluorescence spectrophotometer (Edinburgh Instruments, UK). The excitation wavelength was set at 270 nm, whereas the emission wavelengths were detected from 280 nm to 600 nm at 1 nm steps.

The particle sizes of SMPs in the biofilms were determined by Zetasizer3000HSA nanolaser particle size analyzer (Malvern, UK) after the end of fermentation. The particle size range was 2–3000 nm, and the test temperature was 20 °C. The principle is photon correlation spectroscopy. The liquid sample was

diluted to approach transparency and was ultrasonically treated for 3–5 min, and the particle sizes were then tested.

2.3.4. Gas chromatography analysis

The gas produced from glucose fermentation mainly includes hydrogen, of which the concentration was determined using gas chromatography (GC; Agilent 7820 A, USA) system. GC conducted for 1 min using a 5A molecular sieve column and HayeSep Q column at 65 °C. The temperature was then increased to 145 °C at the rate of 25 °C/min for 1.8 min (argon flow rate was 27 mL/min).

Soluble metabolic degradation byproducts (SMDBs) that mainly contain acetate, ethanol, propionate, isobutyrate, butyrate, isovalerate, valerate, and caproate were analyzed using another GC system (Agilent 7820 A, USA) equipped with a flame ionization detector and DB-FFAP column (Φ 0.32 mm × 50 m, Agilent, USA). The original temperature was maintained at 100 °C for 1 min and then increased to 200 °C at the rate of 10 °C/min for 2.5 min.

2.4. Calculations

The hydrogen yields were simulated using the modified Gompertz equation (Eq. 1), whereas the dynamic parameters were calculated using the Origin 9.0 software. Triplicate experiments for all the conditions were conducted to obtain mean values and standard deviations.

$$H = H_m \exp\left\{-\exp\left[\frac{R_m e}{H_m}(\lambda - t) + 1\right]\right\} \quad (1)$$

where H is the cumulative hydrogen yield, mL/g glucose; H_m is the maximum hydrogen yield potential, mL/g glucose; R_m is the peak rate of hydrogen production,

mL/g glucose/h; and λ is the lag-phase time of hydrogen production, h.

$$T_m = \frac{H_m}{R_m \mathrm{e}} + \lambda \quad (2)$$

where T_m is the peak time, h.

3. Results and discussion

3.1. Microscopic analysis of *E. aerogenes*/HoxEFUYH

The cultures of *E. aerogenes/HoxEFUYH* in supernatant were observed via SEM. As shown in Fig. 1, many nanowires were found between the bacteria in supernatant without carbon cloth. Zhuang et al. found pili on the extracellular membranes of *E. aerogenes*; these pili can serve as electric conduits for electron transfer in spite of insufficient evidence (cyclic voltammograms of bacterial biofilm) [26, 27]. In this study, scarcely any intercellular nanowires were observed after adding carbon cloth by capturing more than 50 SEM images of *E. aerogenes*/HoxEFUYH added with carbon cloth. The representative SEM images are shown as Fig. 1. The carbon cloth possibly replaced pili to act as a conduit among bacteria cells for the electron transfer. The electrical resistivity of carbon cloth is 0.0016 Ω·cm, which is relatively lower than that of most microbial nanowires [28]. Thus, the microorganisms did not have to produce nanowires, thereby reducing the energy consumption for growth.

The SEM images of the carbon cloth on 1 h and 96 h of fermentation were captured to investigate the surface changes in the carbon cloth. Initially, the surface of carbon cloth was smooth and had few microorganisms. At the end of fermentation, the surface was caked with microorganisms, and dense biofilms were formed. Similar

structural changes were reported in carbon nanotubes [29]. The carbon cloth provided an attachment surface for *E. aerogenes/HoxEFUYH* in close contact with each other and facilitated bacteria growth. Thus, the fermentation of glucose was accelerated with the carbon cloth.

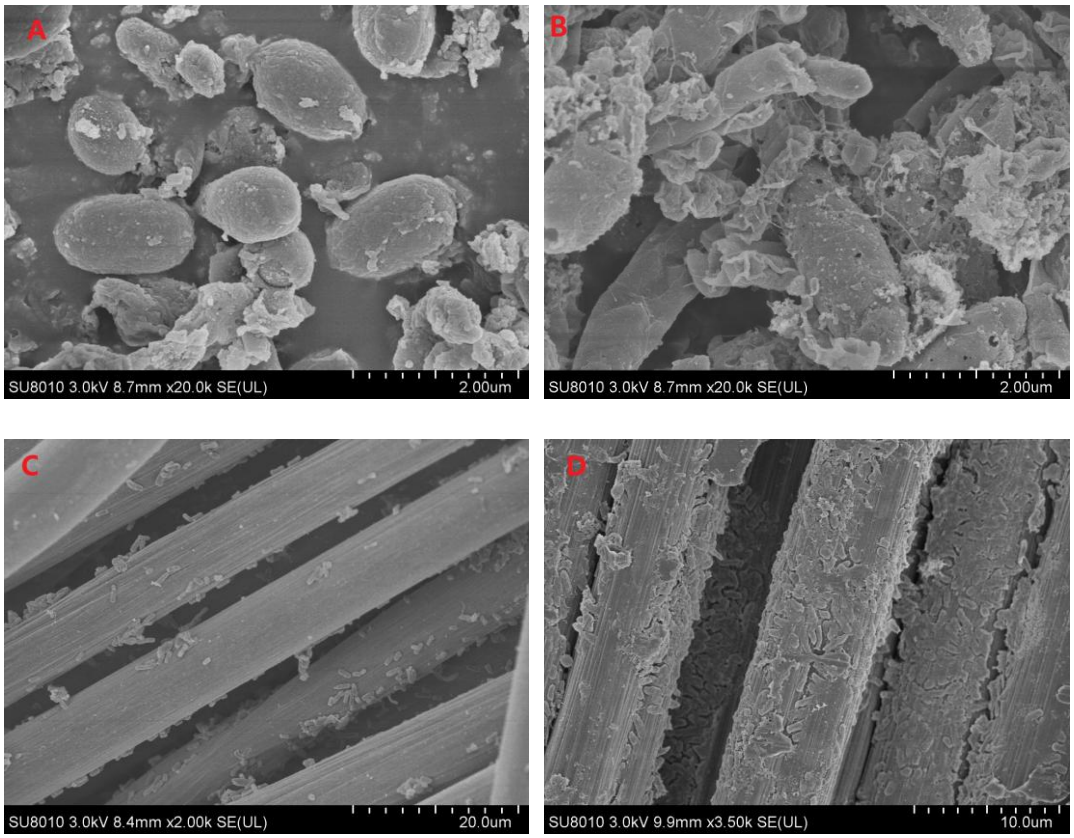

Fig. 1. SEM images of transgenic *E. aerogenes*/HoxEFUYH in the supernatant with/without carbon cloth. (A) *E. aerogenes*/HoxEFUYH in the supernatant with carbon cloth at 20000 ×; (B) *E. aerogenes*/HoxEFUYH without carbon cloth at 20000×; (C) Carbon cloth at 1 h of fermentation at 2000 ×; (D) Carbon cloth at 96 h of fermentation at 3500 ×.

3.2. Analysis of biofilms

3.2.1. Protein contents analysis

At 96 h of fermentation, approximately 59.1% of the microorganisms were firmly attached to the solid particles of carbon fiber, of which the protein content was

approximately 2.6 g/L. By contrast, the protein content in supernatant was 1.8 g/L. The protein content of biofilms attached to cotton cloth was measured as 2.5 g/L, which indicated that the similar proportion of bacteria was immobilized on the cotton cloth. Cell reproduction was promoted by the carbon cloth and cotton cloth because they provided an improved growing environment for the cultures. In addition, the carbon cloth probably substituted for the conducting microbial wires. The energy consumed for microbial growth was reduced, which in turn accelerated the syntrophic metabolism of glucose.

3.2.2. FTIR analysis

FTIR showed the similarities and differences between soluble microbial products (SMPs) from carbon cloth biofilms and supernatant. As shown in Fig. 2, the peaks of SMPs from the biofilms mainly appeared at 3415, 1620, and 1400 cm^{-1}. The absorption bands at 3415 cm^{-1} (O-H) and 1400 cm^{-1} (C-N_2H) were from protein, and that at 1620 cm^{-1} (C=O) was from polysaccharides [30]. Thus, the SMPs in carbon cloth biofilms mainly included large quantities of protein and a small fraction of polysaccharides.

Significant similarities existed between the SMPs in the supernatant and biofilms. In the SMPs from the supernatant, three peaks existed between 800—1200 cm^{-1}, which were ascribed to the C-O stretching vibration in the polysaccharide compound. This finding indicated that polysaccharides occupied a large part of the SMPs in the supernatant as a result of the metabolic substance released from the microorganism. Some deviations existed in peak positions; thereby indicating SMP compositions in the biofilms and supernatant were different.

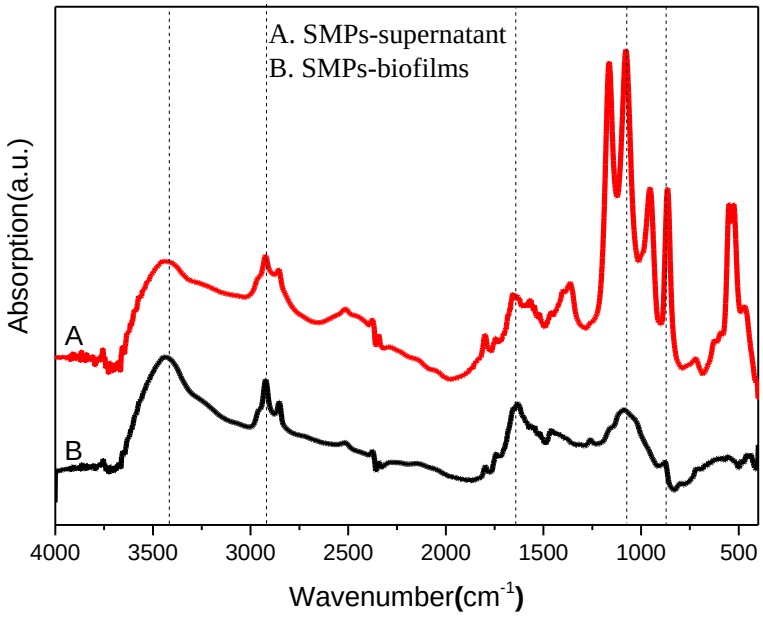

274

275 **Fig. 2.** Fourier transform infrared spectra of soluble microbial products in carbon cloth biofilms

276 and supernatant.

277 **3.2.3. EEM analysis**

278 EEM spectra of SMPs in carbon cloth biofilms and supernatant were tested after

279 fermentation. The results in Fig. 3 reveal that the SMPs in biofilms and supernatant

280 both showed peaks. Compared with supernatant SMPs, biofilm SMPs presented

281 higher intensity peaks, indicating that both of them contained organic matter that

282 could be emitted by fluorescence. However, the organic matter content in biofilm

283 SMPs was higher than that in supernatant. The peak area of fluorescence spectrum

284 can roughly indicate the relative content of fluorescent substances in SMPs. Through

285 peak group analysis and calculation with Origin 9.0, the relative content of fluorescent

286 substances in carbon cloth biofilm SMPs (88.1%) was found to be larger than that in

287 supernatant SMPs (11.9%). In the EEM diagram of the carbon cloth biofilm SMPs,

the location of the peak was concentrated in 357–374 nm, which was associated with soluble microbial by-product-like and humic substance-like substances according to the classification scheme by Chen et al. [31, 32]. Although carbon cloth biofilm SMPs and supernatant SMPs both contained protein substances, their peak positions were different, indicating that the two kinds of proteins contained different species. This result was consistent with FTIR.

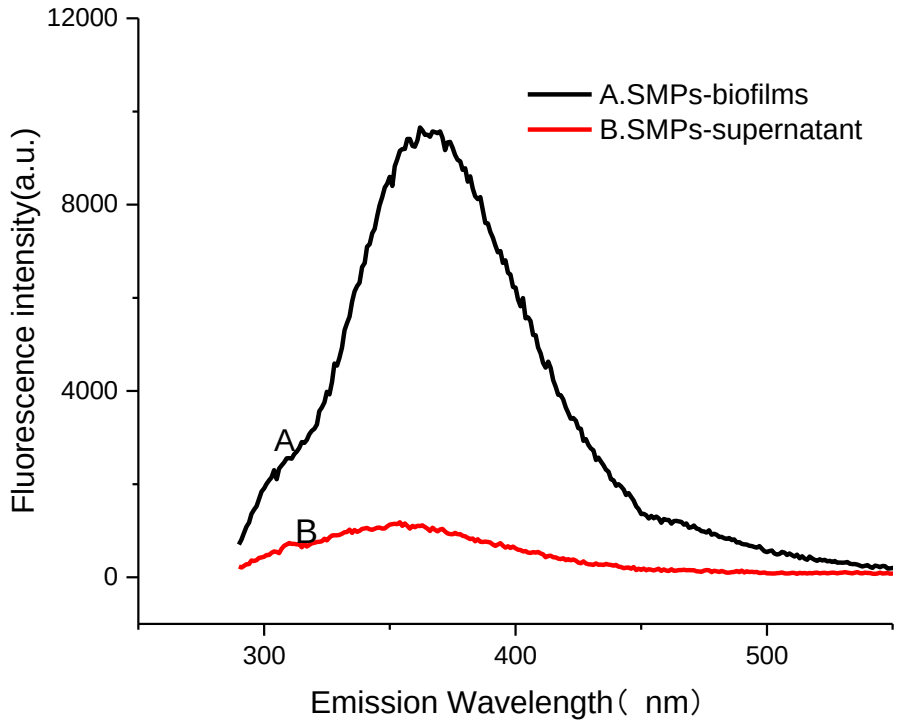

Fig. 3. Excitation Emission Matrix spectra analysis of soluble microbial products in carbon cloth biofilms and supernatant.

3.2.4. Particle size analysis of biofilm SMPs

During fermentation, the organic matter of carbon cloth biofilm SMPs can diffuse into supernatant, thereby promoting the mass transfer between biofilm and

supernatant. The diffusion of macromolecules from biofilm SMPs to supernatant strictly depends on the particle size. The particle sizes of biofilm SMPs at the end of fermentation were determined by volume and quantity as shown in Fig. 4. Different measurement methods showed different particle size distributions. With the volume as the index, the particle size distribution showed three peaks. Molecules from 14 nm to 1000 nm occupied 85.6% of the total particles. Three peaks appeared at 84.3, 395.5, and 1108.8 nm, and the average particle size was 465.2 nm. With the index of number, the peak only appeared at 18 nm. Approximately 98.4% of the molecular sizes were concentrated in 12–200 nm, and the average particle size was 30.2 nm.

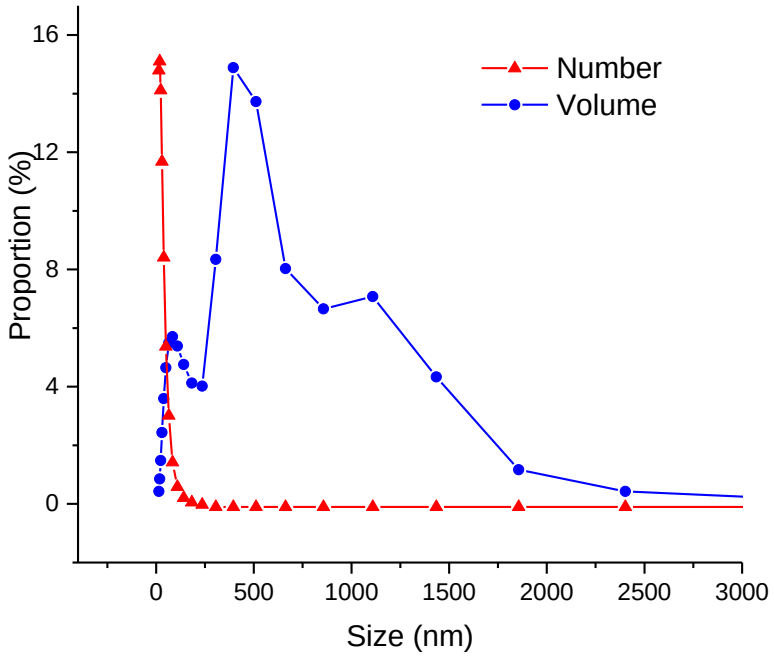

Fig. 4. Particle size distribution of soluble microbial products in carbon cloth biofilms.

The molecular sizes of the carbon cloth biofilm SMPs were less than 1.2 μm. The diameter of carbon cloth fiber is 6.9 μm, and the particle sizes of biofilm SMPs were smaller than those of carbon fiber. This finding indicated that during

fermentation, the substance in biofilm could easily diffuse into the supernatant. These matter and energy flow processes facilitated the hydrogen production by *E. aerogenes*/HoxEFUYH.

3.3. Soluble metabolic degradation products analysis

The total soluble metabolic degradation byproducts (SMDBs) of the dark hydrogen fermentation effluent are shown in Fig. 5. SMDBs included acetate, ethanol, propionate, butyrate, isobutyrate, isovalerate, valerate, and caproate. The acetate (34 mM to 54.5 mM) and ethanol (23 mM to 29 mM) made up most of the liquid products. With 1.0 g/L carbon cloth, the SMDBs increased from 76.9 mM to 107.3 mM. The proportion of ethanol in SMDBs decreased from 29.9% to 27.0%; nevertheless, the proportion of acetate in SMDBs increased from 44.2% to 50.8%. As shown in Eqs. 3 and 4 [33], ethanol pathway theoretically cannot produce hydrogen, whereas acetate pathway can produce 4 mol hydrogen. The metabolic pathways of *E. aerogenes*/HoxEFUYH were changed by accessing suitable carbon cloth, which led to increased acetate and less ethanol levels. The hydrogen production increased correspondingly.

Ethanol pathway: $C_6H_{12}O_6 \rightarrow 2C_2H_5OH+2CO_2$ (3)

Acetic acid pathway: $C_6H_{12}O_6+2H_2O \rightarrow 2CH_3COOH+2CO_2+4H_2$ (4)

The share of propionate in SMDBs decreased from 7.9% to 6.6%. During glucose degradation, pyruvate was first produced through glycolysis; two different metabolic pathways were reported for pyruvate [7]. One is the propionate pathway, in which pyruvate was directly decomposed to propionate without hydrogen production.

The other is the formate pathway, in which pyruvate was degraded into formate, which was then decomposed to hydrogen. The reduction of propionate suggested that proper additions of carbon cloth possibly enhanced the formate pathway and restrained the propionate pathway. As a result, additional hydrogen was obtained.

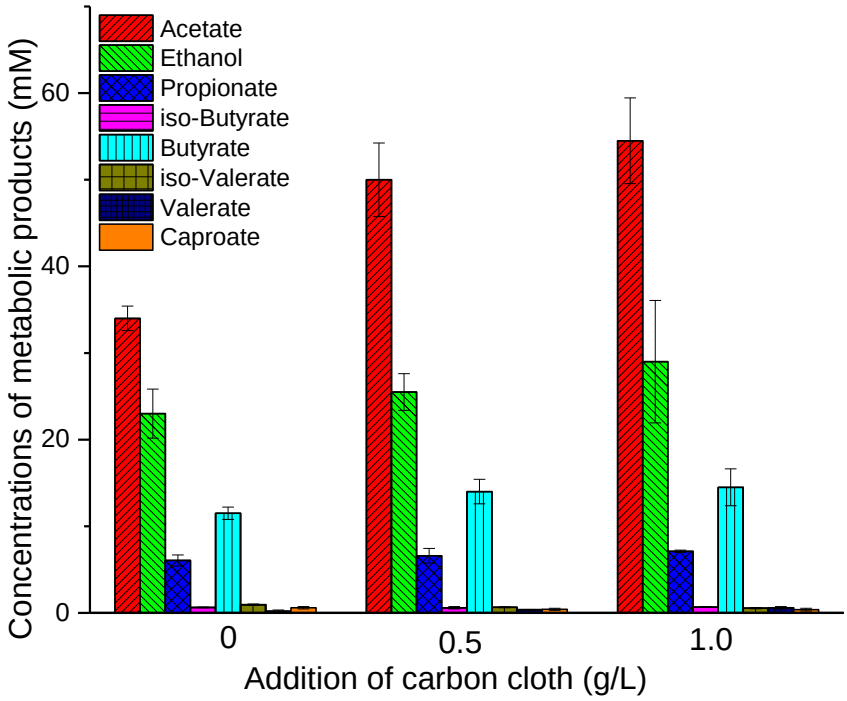

Fig. 5. Soluble metabolic degradation byproducts in hydrogen fermentation of glucose added with carbon cloth.

3.4. Fermentative hydrogen production from glucose

Hydrogen yield (191.3 ± 2.34) was relatively low without any additives. After adding 0.5 and 1.0 g/L carbon cloth, the hydrogen yield reached to 231.7 ± 6.12 and 242.3 ± 2.65 mL/g glucose, respectively (Fig. 6). The highest hydrogen production rate of 11.9 ± 0.10 mL/g/h was achieved in the presence of 1.0 g/L carbon cloth at 36

h. The hydrogen yield also increased to 228.5 ± 3.77 and 236.9 ± 6.35 mL/g glucose in the presence of 0.5 and 1.0 g/L cotton cloth, respectively. The carbon cloth and cotton cloth are favorable to the attachment of micrograms acting as supporting materials and facilitate bacteria growth. As indicated by the analysis of protein contents, the number of microorganisms attached to the surface of carbon or cotton cloth was higher than that in the supernatant. In addition, the enhancement effect on hydrogen production rate of carbon cloth is more evident than of cotton cloth. A possible reason is the carbon cloth can assist the potential electron transfer among hydrogen-producing bacteria, thereby accelerating the metabolism of glucose to hydrogen. Carbon cloth possibly served as electron conduits among bacteria, thus eliminating the need for biological connections such as nanowires. This result was consistent with a previous study, which confirmed that carbon cloth could promote electron transfer [34].

Triplicate experiments for all the conditions were conducted to obtain the average data and their standard deviations. In Fig. 6, error bars represent ± 1 standard deviation of triplicates. Experimental data were evaluated by analysis of variance (ANOVA) applying Tukey test in Origin software at a significance level of 0.05. The P values (Prob>F) are 0.025 and 0.009 in hydrogen yield and hydrogen production rate, which indicate that the differences of results are statistically significant.

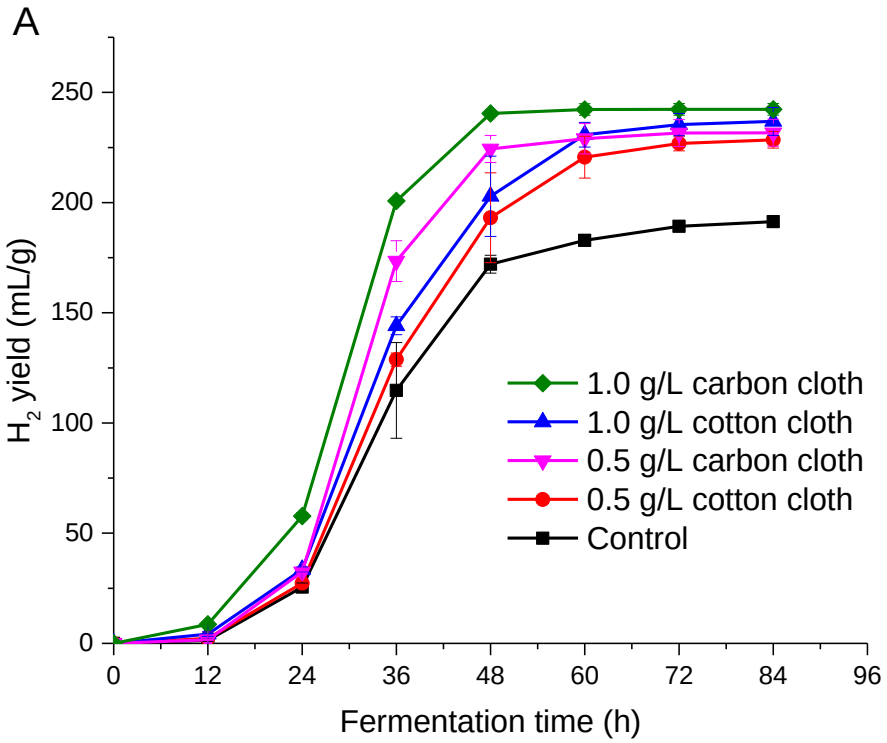

367

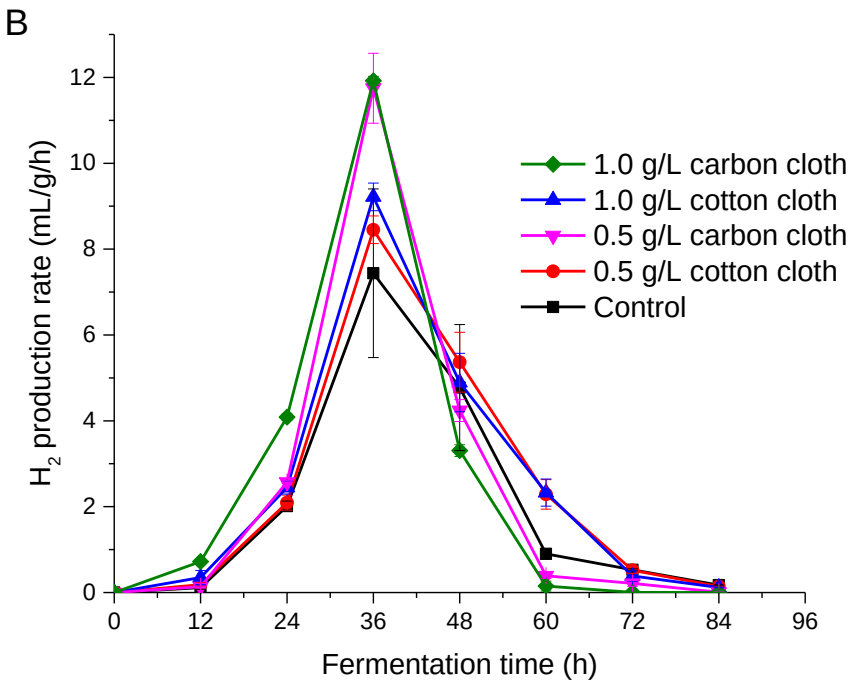

368

369 **Fig. 6.** H_2 production of transgenic *E. aerogenes*/HoxEFUYH with carbon cloth and cotton cloth

370 from glucose. (A) H_2 yield; (B) H_2 production rate.

371 **Table 1.** Dynamic parameters of fermentative H_2 production of transgenic *E.*

372 *aerogenes*/HoxEFUYH with carbon cloth and cotton cloth from glucose.

Additive porous cloth	H_2 yield (mL/g)	H_2 production peak rate (mL/g/h)	Dynamic parameters				
			H_m (mL/g)	R_m (mL/g /h)	λ (h)	T_m (h)	R^2
Control	191.3 ± 2.34	7.44 ± 1.97	190.9	8.3	21.6	30.1	0.9996
0.5 g/L cotton cloth	228.5 ± 3.77	8.45 ± 0.32	229.6	9.0	21.6	31.0	0.9999
1.0 g/L cotton cloth	236.8 ± 6.35	9.22 ± 0.32	237.5	9.6	20.8	30.0	0.9995
0.5 g/L carbon cloth	231.7 ± 6.12	11.7 ± 0.82	231.8	13.7	22.0	28.2	0.9999
1.0 g/L carbon cloth	242.3 ± 2.65	11.9 ± 0.10	243.3	15.2	20.3	26.2	0.9990

373 The kinetic parameters of hydrogen production fitted by the modified Gompertz
374 equation are shown in Table 1. The kinetics of hydrogen production was evaluated in
375 terms of hydrogen yield potential (H_m), peak hydrogen production rate (R_m), lag phase
376 time (λ), and peak time (T_m). The maximum hydrogen yield potential (H_m, 243.3 mL/g)
377 was achieved in the presence of 1.0 g/L carbon cloth, corresponding to a value of 27.4%
378 higher than the control. The lag phase time (λ) and peak time (T_m) were both reduced
379 in the presence of 1.0 g/L carbon cloth. The carbon cloth effectively promoted
380 hydrogen production using *E. aerogenes*/HoxEFUYH. This result was consistent with
381 a previous study, which reported that the hydrogen yield increases with the addition of

biochar [35].

3.5. Proposed mechanisms for enhanced hydrogen production with carbon cloth

As illustrated in Fig. 1, dense microorganism films were formed on the surface of carbon cloth at the end of hydrogen fermentation since the carbon cloth with large surface area is capable of providing support carriers for the attachment and immobilization of bacteria. Furthermore, the analysis of protein content and EEM spectra indicated that microbes attached to the surface of carbon cloth were much denser than those suspended in the supernatant. This kind of cell immobilization technique belongs to surface-attached biofilms [36, 37]. It has been reported that attached cell immobilization is more superior to suspended cell since the fermentation system is more likely to maintain process stability and higher microbial activity [17]. Moreover, the character of porous structure of carbon cloth is favorable of sustaining cell viability, avoiding excess leakage of bacteria and promoting bacterial colonization [17, 36, 38]. Therefore, carbon cloth added in the fermentation system is conducive to create high cell density and efficient hydrogen production.

Apart from having the function of cell immobilization and facilitating biofilm formation, carbon cloth may be capable of promoting the potential bacterial electron transfer. Based on the SEM images of *E. aerogenes/HoxEFUYH* cultures with carbon cloth (Fig. 1), the bacterial nanowires in the supernatant cells almost disappeared with the addition of carbon cloth. The potential approach of electron transfer between cells

403 with nanowires replaced by carbon cloth can be changed. Given that the electrical
404 resistivity of carbon cloth (0.0016 Ω·cm) is lower than that of most microbial
405 nanowires (~0.5 Ω·cm) [28], the electron transport through conductive carbon cloth is
406 likely to be more efficient than through intercellular nanowires.

407 Bacterial communities can exchange cytoplasmic factors, such as proteins [39],
408 nutrients [40], and electrons [41] via intercellular membrane nanotubes. Dubey et al.
409 proposed that nanotube-like membrane structures are major channels of bacterial
410 communication in nature; these channels can offer conduits for exchange of
411 cytoplasmic molecules within and between species [42]. In the current work, the
412 nanowire-like connections between *E. aerogenes*/HoxEFUYH cells possibly serve as
413 communication channels to exchange electrons. As exoelectrogenic bacteria, *E.*
414 *aerogenes* have been applied in the field of microbial fuel cells (MFCs) for a long
415 time; previous studies indicated that the current generation is not only attributed to
416 situ biohydrogen oxidization but is also related to direct electroactive biofilms [6].
417 Reguera et al. also reported that *E. aerogenes* might directly transfer electrons to the
418 electrode via the electroconductive pili on their external membranes in biofilms [43].
419 In summary, the electron exchange between neighboring cells via conjugative
420 nanowires is a possible form of bacterial communication.

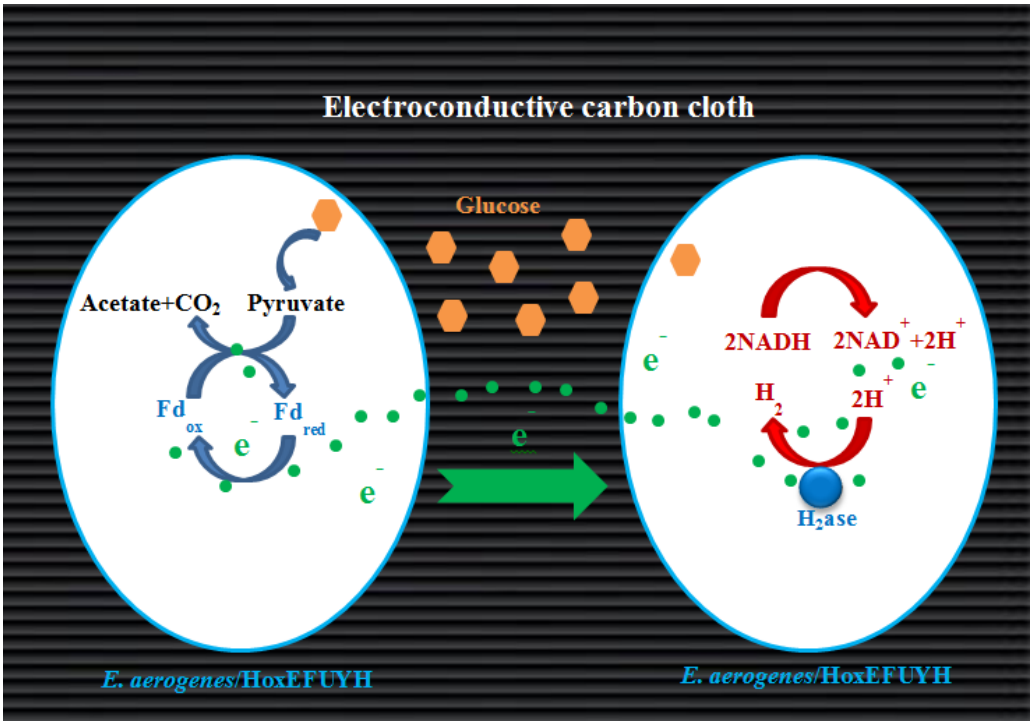

421

422 **Fig. 7.** Schematic diagram of the proposed mechanism for enhancing electron transfer between

423 transgenic *E. aerogenes*/HoxEFUYH cells with conductive carbon cloth.

424 In this study, many bacterial nanowires were observed in the SEM images of *E.*

425 *aerogenes*/HoxEFUYH without carbon cloth (Fig. 1B). These nanowires can serve as

426 electric conduits for the electron transfer among *E. aerogenes*/HoxEFUYH cells.

427 Almost no bacterial nanowires were observed in the supernatant cells due to the

428 presence of conductive carbon cloth (Fig. 1A). As illustrated in Fig. 7, it is likely that

429 the carbon cloth replaced nanowires to act as a conduit among bacteria for the

430 electron transfer. The primary hydrogen synthesis process in *E.*

431 *aerogenes/HoxEFUYH* cell could be characterized as follows: glucose degraded to

432 pyruvate, which was converted to acetylCoA, which can be further decomposed into

433 acetate, and ferredoxin can be reduced by NADH: ferredoxin oxidoreductase (NFOR)

434 [3, 44]. In view of the potential interactions and electron transport within *E. aerogenes*

435 species, the electrons released from reduced ferredoxin are likely to be transferred
436 across the cell membrane to the hydrogenase in an adjacent cell through carbon cloth.
437 This process aims to reduce the protons provided by NADH to molecular hydrogen, in
438 case the ferredoxin could not instantly feed sufficient electrons to hydrogenase in the
439 electron-accepting cell. The rate of intercellular electron transfer is likely to be
440 enhanced with carbon cloth because the electrical resistivity (0.0016 Ω·cm) of which
441 is lower than that of most microbial nanowires [28]. Thus, hydrogen production rate
442 increased with proton reduction efficiency. In summary, the carbon cloth potentially
443 promoted hydrogen production by accelerating the electron transfer among *E.*
444 *aerogenes*/HoxEFUYH cells.
445
446 **4. Conclusions**
447 This study reported that conductive carbon cloth can facilitate dark hydrogen
448 fermentation potentially due to the enhancement of intercellular electron transfer
449 among *E. aerogenes* cells. Carbon cloth provided a sufficient place for bacterial
450 attachment, which led to the biofilm growth with 59.1% of the total microorganism
451 population. SEM showed the disappearance of bacterial nanowires, suggesting that
452 carbon cloth possibly replaced bacterial nanowires to serve as electron conduits. FTIR
453 analysis revealed that SMPs in carbon cloth biofilms mainly contained
454 polysaccharides, proteins, and humic-like substances. EEM indicated that the relative
455 content of fluorescent substances in biofilm SMPs (88.1%) is larger than that in

supernatant SMPs (11.9%). Metabolic analysis revealed that carbon cloth stimulated acetate pathway but impaired ethanol pathway. While this study displays the feasibility of using conductive carbon cloth to promote hydrogen fermentation, the mechanism of bacterial communication and electron transfer in the presence of carbon cloth need to be further investigated.

Acknowledgements

This study was supported by the National Key Research and Development Program-China (2016YFE0117900), and Zhejiang Provincial Key Research and Development Program-China (2017C04001). Dr. Richen Lin gratefully acknowledges the support from the European Union's Horizon 2020 research and innovation programme under the Marie Skłodowska-Curie grant agreement No 797259.

References

[1] Navarro-Díaz M, Valdez-Vazquez I, Escalante AE. Ecological perspectives of hydrogen fermentation by microbial consortia: What we have learned and the way forward. Int J Hydrogen Energy 2016;41:17297-308.

[2] Kothari R, Singh DP, Tyagi VV, Tyagi SK. Fermentative hydrogen production – An alternative clean energy source. Renew Sustain Energy Rev 2012;16:2337-46.

[3] Hallenbeck PC. Fermentative hydrogen production: Principles, progress, and prognosis. Int J Hydrogen Energy 2009;34:7379-89.

[4] Christopher K, Dimitrios R. A review on exergy comparison of hydrogen production methods from renewable energy sources. Energy Environ Sci 2012;5:6640-51.

[5] Xia A, Jacob A, Herrmann C, Tabassum MR, Murphy JD. Production of hydrogen, ethanol and volatile fatty acids from the seaweed carbohydrate mannitol. Bioresour Technol 2015;193:488-97.

[6] Zhang C, Lv FX, Xing XH. Bioengineering of the *Enterobacter aerogenes* strain for biohydrogen production. Bioresour Technol 2011;102:8344-9.

[7] Cai GQ, Jin B, Monis P, Saint C. Metabolic flux network and analysis of fermentative hydrogen production. Biotechnol Adv 2011;29:375-87.

[8] Zhang C, Ma K, Xing XH. Regulation of hydrogen production by *Enterobacter aerogenes* by external NADH and NAD^+. Int J Hydrogen Energy 2009;34:1226-32.

[9] Zhao J-F, Song W-L, Cheng J, Zhang C-X. Heterologous expression of a hydrogenase gene in *Enterobacter aerogenes* to enhance hydrogen gas production. World J Microbiol Biotechnol 2010;26:177-81.

[10] Mishra P, Das D. Biohydrogen production from *Enterobacter cloacae* IIT-BT 08 using distillery effluent. Int J Hydrogen Energy 2014;39:7496-507.

[11] Nasr M, Tawfik A, Ookawara S, Suzuki M, Kumari S, Bux F. Continuous biohydrogen production from starch wastewater via sequential dark-photo fermentation with emphasize on maghemite nanoparticles. J Ind Eng Chem 2015;21:500-6.

[12] Gadhe A, Sonawane SS, Varma MN. Enhancement effect of hematite and nickel nanoparticles on biohydrogen production from dairy wastewater. Int J Hydrogen Energy 2015;40:4502-11.

[13] Beckers L, Hiligsmann S, Lambert SD, Heinrichs B, Thonart P. Improving effect of metal and oxide nanoparticles encapsulated in porous silica on fermentative biohydrogen production by *Clostridium butyricum*. Bioresour Technol 2013;133:109-17.

[14] Taherdanak M, Zilouei H, Karimi K. The effects of Fe^0 and Ni^0 nanoparticles versus Fe^{2+} and Ni^{2+} ions on dark hydrogen fermentation. Int J Hydrogen Energy 2016;41:167-73.

[15] Zhang Y, Shen J. Enhancement effect of gold nanoparticles on biohydrogen production from artificial wastewater. Int J Hydrogen Energy 2007;32:17-23.

[16] Zhang J, Fan C, Zang L. Improvement of hydrogen production from glucose by ferrous iron and biochar. Bioresour Technol 2017;245:98-105.

[17] Jamali NS, Jahim JM, Wan NRWI. Biofilm formation on granular activated carbon in xylose and glucose mixture for thermophilic biohydrogen production. Int J Hydrogen Energy 2016;41:21617-27.

[18] Elreedy A, Ibrahim E, Hassan N, El-Dissouky A, Fujii M, Yoshimura C, et al. Nickel-graphene nanocomposite as a novel supplement for enhancement of biohydrogen production from industrial wastewater containing mono-ethylene glycol. Energy Convers Manage 2017;140:133-44.

519 [19] Liu W, Cheng S, Guo J. Anode modification with formic acid: A simple and
520 effective method to improve the power generation of microbial fuel cells. Appl Surf
521 Sci 2014;320:281-6.
522 [20] Liu F, Rotaru AE, Shrestha PM, Malvankar NS, Nevin KP, Lovley DR.
523 Promoting direct interspecies electron transfer with activated carbon. Energy Environ
524 Sci 2012;5:8982-9.
525 [21] Song W, Cheng J, Zhao J, Carrieri D, Zhang C, Zhou J, et al. Improvement of
526 hydrogen production by over-expression of a hydrogen-promoting protein gene in
527 *Enterobacter cloacae*. Int J Hydrogen Energy 2011;36:6609-15.
528 [22] Wang X, Cheng S, Feng Y, Merrill MD, Saito T, Logan BE. Use of Carbon Mesh
529 Anodes and the Effect of Different Pretreatment Methods on Power Production in
530 Microbial Fuel Cells. Environ Sci Technol 2009;43:6870-4.
531 [23] Zhu N, Chen X, Zhang T, Wu P, Li P, Wu J. Improved performance of membrane
532 free single-chamber air-cathode microbial fuel cells with nitric acid and
533 ethylenediamine surface modified activated carbon fiber felt anodes. Bioresour
534 Technol 2011;102:422-6.
535 [24] Kunacheva C, Yan NAS, Trzcinski AP, Stuckey DC. Soluble Microbial Products
536 (SMPs) in the Effluent from a Submerged Anaerobic Membrane Bioreactor (SAMBR)
537 under Different HRTs and Transient Loading Conditions. Chem Eng J
538 2017;311:72-81.
539 [25] Cheng J, Lin R, Ding L, Song W, Li Y, Zhou J, et al. Fermentative hydrogen and

methane cogeneration from cassava residues: Effect of pretreatment on structural characterization and fermentation performance. Bioresour Technol 2014;179:407-13.

[26] Venkataraman A, Rosenbaum MA, Perkins SD, Werner JJ, Angenent LT. Metabolite-based mutualism between *Pseudomonas aeruginosa* PA14 and *Enterobacter aerogenes* enhances current generation in bioelectrochemical systems. Energy Environ Sci 2011;4:4550-9.

[27] Zhuang L, Zhou SG, Yuan Y, Liu TL, Wu ZF, Cheng J, et al. Development of *Enterobacter aerogenes* fuel cells: from in situ biohydrogen oxidization to direct electroactive biofilm. Bioresour Technol 2011;102:284-9.

[28] LampaPastirk S, Veazey JP, Walsh KA, Feliciano GT, Steidl RJ, Tessmer SH, et al. Thermally activated charge transport in microbial protein nanowires. Sci Rep 2016;6:23517.

[29] Li LL, Tong ZH, Fang CY, Chu J, Yu HQ. Response of anaerobic granular sludge to single-wall carbon nanotube exposure. Water Res 2015;70:1-8.

[30] Nam AT, Cheng NG, May CAS, Gyu LM. Elucidation of the effect of ionic liquid pretreatment on rice husk via structural analyses. Biotechnol Biofuels 2012;5:1-10.

[31] Chen W, Westerhoff P, Leenheer JA, Booksh K. Fluorescence excitation-emission matrix regional integration to quantify spectra for dissolved organic matter. Environ Sci Technol 2003;37:5701-10.

[32] Ramesh A, Lee DJ, Lai JY. Membrane biofouling by extracellular polymeric substances or soluble microbial products from membrane bioreactor sludge. Appl

561 Microbiol Biotechnol 2007;74:699-707.

562 [33] Azwar MY, Hussain MA, Abdul-Wahab AK. Development of biohydrogen
563 production by photobiological, fermentation and electrochemical processes: A review.
564 Renew Sustain Energy Rev 2014;31:158-73.

565 [34] Chen S, Rotaru A-E, Liu F, Philips J, Woodard TL, Nevin KP, et al. Carbon cloth
566 stimulates direct interspecies electron transfer in syntrophic co-cultures. Bioresour
567 Technol 2014;173:82-6.

568 [35] Luo C, Lü F, Shao L, He P. Application of eco-compatible biochar in anaerobic
569 digestion to relieve acid stress and promote the selective colonization of functional
570 microbes. Water Res 2015;68:710-8.

571 [36] Gokfiliz P, Karapinar I. The effect of support particle type on thermophilic
572 hydrogen production by immobilized batch dark fermentation. Int J Hydrogen Energy
573 2017;42:2553-61.

574 [37] Cappelletti M, Bucchi G, Mendes JDS, Alberini A, Fedi S, Bertin L, et al.
575 Biohydrogen production from glucose, molasses and cheese whey by suspended and
576 attached cells of four hyperthermophilic Thermotoga strains. J Chem Technol
577 Biotechnol 2012;87:1291-301.

578 [38] Barca C, Soric A, Ranava D, Giudiciorticoni MT, Ferrasse JH. Anaerobic biofilm
579 reactors for dark fermentative hydrogen production from wastewater: A review.
580 Bioresour Technol 2015;185:386-98.

581 [39] Ducret A, Fleuchot B, Bergam P, Mignot T. Direct live imaging of cell–cell

582 protein transfer by transient outer membrane fusion in *Myxococcus xanthus*. Elife
583 2013;2:e00868.
584 [40] Pande S, Shitut S, Freund L, Westermann M, Bertels F, Colesie C, et al.
585 Metabolic cross-feeding via intercellular nanotubes among bacteria. Nat Commun
586 2015;6:1-13.
587 [41] Pirbadian S, Barchinger SE, Leung KM, Byun HS, Jangir Y, Bouhenni RA, et al.
588 *Shewanella oneidensis* MR-1 nanowires are outer membrane and periplasmic
589 extensions of the extracellular electron transport components. Proc Natl Acad Sci U S
590 A 2014;111:12883-8.
591 [42] Dubey, Gyanendra P, BenYehuda, Sigal. Intercellular Nanotubes Mediate
592 Bacterial Communication. Cell 2011;144:590-600.
593 [43] Reguera G, Mccarthy KD, Mehta T, Nicoll JS, Tuominen MT, Lovley DR.
594 Extracellular Electron Transfer Via Microbial Nanowires. Nature 2005;435:1098-101.
595 [44] Hsieh PH, Lai YC, Chen KY, Hung CH. Explore the possible effect of TiO_2 and
596 magnetic hematite nanoparticle addition on biohydrogen production by *Clostridium*
597 *pasteurianum* based on gene expression measurements. Int J Hydrogen Energy
598 2016;41:21685-91.
599